Slow decay of the finite Reynolds number effect of turbulence

J. Qian
Department of Physics, Graduate School of Academia Sinica, P.O. Box 3908, Beijing 100039, China
(Received 5 November 1998)

The third-order structure function is used to study the finite Reynolds number (FRN) effect of turbulence, which refers to the deviation of turbulence statistics observed at finite Reynolds numbers from predictions of the Kolmogorov theories. It is found that the FRN effect decreases as $CR_\lambda^{-\mu}$, when R_λ is high, and $\mu \leqslant 6/5$. Here R_λ is the Taylor-microscale Reynolds number and C is a constant independent of R_λ. From the exact spectral equations, the decay exponent μ and the constant C are determined for typical fully developed turbulent flows (freely decaying isotropic turbulence and shear flow turbulence), so that the quantitative prediction of the FRN effect is feasible. [S1063-651X(99)05408-2]

PACS number(s): 47.27.Gs, 47.27.Jv

The Kolmogorov theories, which correspond to the asymptotic case of infinite Reynolds number, have profoundly shaped and illuminated thinking about turbulence [1]. However, experiments and numerical simulations are made at finite Reynolds numbers. The finite Reynolds number (FRN) effect of turbulence refers to the deviation of turbulence statistics observed at finite Reynolds numbers from predictions of the Kolmogorov theories [2]. Let R_λ be the Taylor-microscale Reynolds number. It is commonly assumed that the FRN effect decays quite fast as R_λ increases and can be neglected at experimental R_λ (10^2-10^3), so the turbulence statistics observed in experiments and simulations can be described by the Kolmogorov theories [3]. In fact, in many cases, this assumption is not reasonable and leads to a faulty interpretation of data [2,4]. In order to decide whether the FRN effect is important at given R_λ, it is necessary to study how the FRN effect decays as R_λ increases. In this paper, from exact spectral equations, we derive the decay law of the FRN effect and determine all relevant constants for typical fully developed turbulent flows, so that the quantitative prediction of the FRN effect is feasible. The study of the FRN effect helps to resolve many issues in the statistical physics of turbulence.

In the inertial range, the third-order structure function $D_{LLL}(r)$ becomes [3]

$$D_{LLL}(r) = -(4/5)\varepsilon r \quad \text{or} \quad -D_{LLL}(r)/\varepsilon r = 0.8, \tag{1}$$

which is Kolmogorov's 4/5 law. Here, r is the distance and ε is the energy dissipation rate. From Eq. (1), $D_{LLL}(r)$ scales as r in the inertial range, so the popular method of finding the inertial range in experiments is to make a log-log plot of $D_{LLL}(r)$ against r, and then the approximate $D_{LLL}(r) \sim r$ scaling range in the plot is taken as the inertial range [5]. For example, the scaling range is about one decade at $R_\lambda = 800$ [5]. However, in the so-called inertial range observed at experimental R_λ, Eq. (1) is not valid, since $-D_{LLL}(r)/\varepsilon r$ is substantially less than 0.8 and is not a constant independent of r [2]. Hence, the approximate $D_{LLL}(r) \sim r$ scaling range found at experimental R_λ, which is commonly called the inertial range in the literature, actually is not the real inertial range, and will be called the scaling range in this paper to distinguish it from the real inertial range. Let

$$y = -D_{LLL}(r)/\varepsilon r \quad \text{and} \quad x = \log_{10}(r/\eta), \tag{2}$$

where $\eta = (\nu^3/\varepsilon)^{1/4}$ is the Kolmogorov length scale and ν is the kinematic viscosity. The curvature of the curve of $y(x)$ in the x-y plane is

$$C_R = d^2y/dx^2/[1+(dy/dx)^2]^{3/2}. \tag{3}$$

The 4/5 law (1) corresponds to the horizontal line $y = 0.8$ in the x-y plane, and its curvature $C_R = 0$. For the scaling range observed at experimental R_λ, the curve of $y(x)$ is below the line $y = 0.8$, and the shortest distance from the curve to the horizontal line $y = 0.8$ of the inertial range is

$$\delta = 0.8 - y(x_m) = 0.8 - \text{maximum of } [-D_{LLL}(r)/\varepsilon r]. \tag{4}$$

y attains its maximum $y(x_m)$ at $x_m = \log_{10}(r_m/\eta)$. The curvature at x_m is negative, and its absolute value is (dy/dx at $x = x_m$ is zero)

$$\phi = |C_R(x_m)| = |d^2y/dx^2 \text{ at } x = x_m|. \tag{5}$$

Since we know the exact inertial-range relation (1) for $D_{LLL}(r)$, it is convenient to use $D_{LLL}(r)$ to study the finite Reynolds number (FRN) effect, and the shortest distance δ and the curvature ϕ are the proper measure of the FRN effect. We will prove that δ and ϕ have the same decay exponent $\mu \leqslant \frac{6}{5}$,

$$\delta = C_\delta R_\lambda^{-\mu} \quad \text{and} \quad \phi = C_\phi R_\lambda^{-\mu} \quad \text{if } R_\lambda \gg 1. \tag{6}$$

μ, C_δ, and C_ϕ will be determined for typical fully developed turbulent flows.

By a similar process of deriving Eq. (12.141) of the Monin-Yaglom (MY) book [3], we have

$$y = -D_{LLL}(r)/\varepsilon r = 12\int_0^\infty G(k)[z^2\sin(z) + 3z\cos(z) - 3\sin(z)]/z^6 dz, \quad z = kr, \tag{7}$$

$$G(k) = kT(k)/\varepsilon, \tag{8}$$

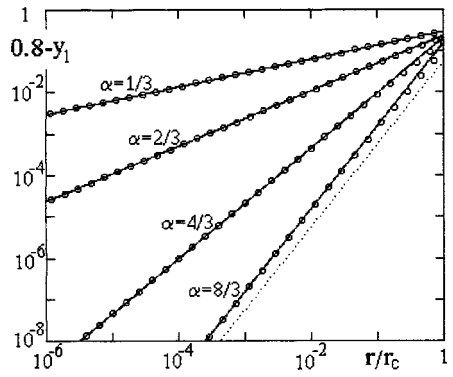

FIG. 1. Log-log plot of $(0.8-y_1)$ vs r/r_c for Eq. (21a) with $\gamma=2$ and $\alpha=\frac{1}{3}$, $\frac{2}{3}$, $\frac{4}{3}$, and $\frac{8}{3}$. ○ ○ ○, numerical results; ——, Eq. (22); ·····, $\alpha=\infty$ or the δ-function model (23). The diagram for $\gamma=5$ or 20 is similar.

where $T(k)$ is the energy transfer spectrum function and $G(k)$ is a dimensionless function. Generally speaking, $G(k)$ or $T(k)$ has the additive property

$$G(k)=G_1+G_2, \quad G_2=2\nu k^3E(k)/\varepsilon. \tag{9}$$

Here $E(k)$ is the three-dimensional energy spectrum and G_2 corresponds to the energy dissipation at small scales due to viscosity. The G_1 corresponds to the energy input at large scales, and its form is derived for the following typical cases of fully developed turbulence.

Case (i). Freely decaying isotropic turbulence. The spectral equation is

$$\partial E(k)/\partial t+2\nu k^2E(k)=T(k), \tag{10}$$

(see the MY book [3]). From Eqs. (8), (9), and (10), we have

$$G_1=k(\partial E(k)/\partial t)/\varepsilon. \tag{11}$$

Case (ii). Homogeneous shear flow turbulence. The coordinates (x_1,x_2,x_3) are chosen in such a way that the main parallel flow is along the x_1 direction and has a constant velocity gradient $S=dU_1(x_2)/dx_2$. The spectral equation is [6]

$$T(k)=S\{4\pi k^2[E_{12}]_{\rm av}-2\pi k^2[k_1\partial E_{ii}/\partial k_2]_{\rm av}\}+2\nu k^2E(k). \tag{12}$$

Here E_{ij} is the spectrum tensor, $E_{ii}=E_{11}+E_{22}+E_{33}$ is its contraction, and $[\ ]_{\rm av}$ means Batchelor's average. In isotropic turbulence, the correlation or spectrum functions depends on one single scalar only, namely the distance r or the wave number k. However, that is no longer valid in the nonisotropic case. Batchelor suggested averaging the correlation or spectrum functions over all directions of r or k, and then the resultant average functions depend on r or k only. Moreover, important relations of isotropic turbulence statistics are also valid for these average functions of nonisotropic turbulence [6]. In Eq. (12), $T(k)$ and $E(k)$ are also Batchelor's average functions [6]. From Eqs. (8), (9), and (12), we have

$$G_1=Sk\{4\pi k^2[E_{12}]_{\rm av}-2\pi k^2[k_1\partial E_{ii}/\partial k_2]_{\rm av}\}/\varepsilon. \tag{13}$$

A linear transform from $G(k)$ to $y(r)$ is defined by Eq. (7) and is denoted by Ψ. By using the additive property (9), we have

$$y=\Psi[G]=y_1+y_2, \quad y_1=\Psi[G_1],$$

$$y_2=\Psi[G_2]=\Psi[2\nu k^3E(k)/\varepsilon]. \tag{14}$$

Let L be the characteristic large scale and $k_d=1/\eta$ be the Kolmogorov wave number. In the universal range $k\gg 1/L$, we have [3,6]

$$E(k)=K_0\varepsilon^{2/3}k^{-5/3}F(k/k_d), \quad F(0)=1, \tag{15}$$

where K_0 is the Kolmogorov constant. The energy relationship is

$$\int_0^\infty 2\nu k^2E(k)dk=\varepsilon \quad \text{or} \quad \int_0^\infty G_2/k dk=1. \tag{16}$$

From Eqs. (7), (14), (15), and (16), we obtain

$$y_2=-C_2(r/\eta)^{-4/3} \quad \text{if} \quad \eta\ll r\ll L, \tag{17a}$$

$$C_2=(324/55)\Gamma(\tfrac{4}{3})K_0=5.26K_0, \tag{17b}$$

which can also be derived by Kolmogorov's equation; Γ is the Gamma function.

Now we study $y_1=\Psi[G_1]$. Since $\int_0^\infty T(k)dk=0$, from Eqs. (8), (9), and (16), we have

$$\int_0^\infty G/k\,dk=0 \quad \text{and} \quad \int_0^\infty G_1/k\,dk=-1, \tag{18}$$

hence $G_1(0)=0$. In the scaling range, $1/L\ll k\ll k_d$,

$$G_1\sim k^{-\alpha}, \tag{19}$$

where the exponent α depends upon the type of turbulence and is determined later. By Eq. (18), the characteristic wave number k_c of energy input is defined by

$$\int_0^{k_c} G_1/k\,dk=\int_{k_c}^\infty G_1/k\,dk=-\tfrac{1}{2}. \tag{20}$$

Various reasonable models of G_1, compatible with Eqs. (18) and (19) and $G_1(0)=0$, have been tested, for example (using a proper unit of k, which is of order $1/L$):

$$G_1(k)=C_Nk^\gamma/(1+k^{\alpha+\gamma}),$$

$$C_N \text{ is determined by Eq. (18);} \tag{21a}$$

$$G_1(k)=0 \quad \text{if } k<1, \quad G_1(k)=-\alpha k^{-\alpha} \quad \text{if } k\geqslant 1; \tag{21b}$$

$$G_1(k)=C_N\exp[-(\beta/k)^\gamma]k^{-\alpha},$$

$$C_N \text{ is determined by Eq. (18);} \tag{21c}$$

$$G_1(k)=C_Nk^\gamma \quad \text{if } k<1, \quad G_1(k)=C_Nk^{-\alpha} \quad \text{if } k\geqslant 1; \tag{21d}$$

TABLE I. Coefficient C_1 in Eq. (22) for various models of G_1.

Model of G_1	$\alpha=\frac{1}{3}$ $(m=\frac{1}{3})$	$\alpha=\frac{2}{3}$ $(m=\frac{2}{3})$	$\alpha=\frac{4}{3}$ $(m=\frac{4}{3})$
Eq. (21a), $\gamma=2$	0.297	0.236	0.212
Eq. (21a), $\gamma=5$	0.297	0.232	0.192
Eq. (21a), $\gamma=20$	0.297	0.232	0.190
Eq. (21b)	0.297	0.232	0.190
Eq. (21c), $\gamma=2$, $\beta=\frac{1}{2}$	0.297	0.237	0.218
Eq. (21c), $\gamma=2$, $\beta=2$	0.297	0.237	0.218
Eq. (21d), $\gamma=2$	0.297	0.232	0.189
Eq. (21d), $\gamma=20$	0.297	0.232	0.190

C_N is a normalization factor determined by Eq. (18). By Eqs. (7), (14), and (21), we calculate $y_1=\Psi[G_1]$ numerically. A log-log plot of $(0.8-y_1)$ versus r/r_c is given in Fig. 1 for Eq. (21a), where $r_c=1/k_c$ and is determined by Eq. (20). The same diagram as Fig. 1 is obtained for Eq. (21b) or Eq. (21c) or Eq. (21d). In summary, we have

$$0.8-y_1=C_1(r/r_c)^m \quad \text{if } r\ll r_c, \quad r_c=1/k_c, \tag{22a}$$

$$m=\alpha \quad \text{if } \alpha<2 \quad \text{and} \quad m=2 \quad \text{if } \alpha>2. \tag{22b}$$

The coefficient C_1 is determined by the least-squares method for $r/r_c\ll 1$, and is given in Table I for various models of G_1. Table I shows that C_1 mainly depends on α, and the behavior of G_1 around k_c has little effect on y_1 at $r\ll r_c$. The expression of the dotted line in Fig. 1 is

$$0.8-y_1=(2/35)(r/r_c)^2, \tag{23a}$$

which corresponds to $\alpha=\infty$ or the Dirac δ-function model of energy input, i.e.,

$$G_1(k)=-k\delta(k-k_c). \tag{23b}$$

From Eqs. (2), (14), (17), and (22), we obtain the important relation

$$y=-D_{LLL}(r)/\varepsilon r=0.8-C_1(r/r_c)^m-C_2(r/\eta)^{-4/3} \quad \text{if } \eta\ll r\ll r_c. \tag{24}$$

Hence, strictly speaking, the 4/5 law (1) is valid only for the case of $r_c/\eta\to\infty$ (i.e., $R_\lambda\to\infty$). The last two terms of Eq. (24) correspond to the FRN effect. $C_1>0$ and $C_2>0$, so $-D_{LLL}(r)/\varepsilon r$ must be less than $\frac{4}{5}$ in the scaling range at a finite R_λ.

Now we determine the exponents α and m of Eqs. (19) and (22). In case (i), freely decaying isotropic turbulence, G_1 is given by Eq. (11); at the stage of self-preservation of the energy spectrum in the universal equilibrium range, a steady $k^{-5/3}$ scaling range is observed, so $[\partial E(k)/\partial t]\sim k^{-5/3}$ in the scaling range, and we have

$$G_1\sim k^{-\alpha}, \quad \alpha=\tfrac{2}{3} \quad \text{for the case (i).} \tag{25}$$

In case (ii), the term $4\pi k^2[E_{12}]_{\text{av}}$ in Eq. (13) corresponds to the shear stress cospectrum $E_{12}(k)$ of [7], and its decay is not more rapid than $k^{-7/3}$ in the $k^{-5/3}$ scaling range [7], i.e., $4\pi k^2[E_{12}]_{\text{av}}\sim k^{-\zeta}$ $(\zeta\leqslant\frac{7}{3})$. The term $k^2[k_1\partial E_{ii}/\partial k_2]_{\text{av}}$ in Eq. (13) equals $\partial\{k[k_1k_2E_{ii}]_{\text{av}}\}/\partial k$, and its decay is not slower than $E(k)=2\pi k^2[E_{ii}]_{\text{av}}$ [6], so $k^2[k_1\partial E_{ii}/\partial k_2]_{\text{av}}\sim k^{-\zeta}$ $(\zeta\geqslant\frac{5}{3})$ in the $k^{-5/3}$ scaling range. From Eq. (13), we conclude that in the scaling range of homogeneous shear flow turbulence,

$$G_1\sim k^{-\alpha}, \quad \tfrac{2}{3}\leqslant\alpha\leqslant\tfrac{4}{3}, \tag{26}$$

which is expected to be applicable in the $k^{-5/3}$ scaling range of an inhomogeneous turbulence at a high R_λ, since the inhomogeneous effect is negligible in the small-scale range. According to Lumley's work [8], in the wall turbulence, the additive property (9) is also valid and G_1 also contains the terms of Eq. (13).

By Eqs. (2)–(5) and (24), it is easy to express the shortest distance δ and the curvature ϕ in terms of r_c/η, but it is

TABLE II. μ, C_δ, and C_ϕ in Eqs. (6) and (29) for typical α and K_0.

	$\alpha=\frac{2}{3}$ $(m=\frac{2}{3})$, $\mu=\frac{2}{3}$		$\alpha=\frac{4}{3}$ $(m=\frac{4}{3})$, $\mu=1$	
K_0	C_δ	C_ϕ	C_δ	C_ϕ
1.2	5.4±0.4	25±2	18±2	175±15
1.5	6.8±0.4	32±2	25±3	243±22
1.8	8.1±0.5	38±3	34±3	320±28

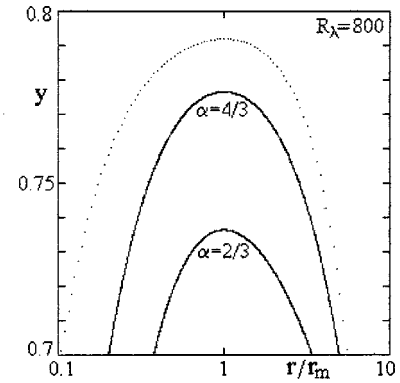

FIG. 2. Linear-log plot of $y=-D_{LLL}(r)/\varepsilon r$ vs r/r_m for $R_\lambda=800$; y attains its maximum $y(r_m)$ at $r=r_m$, $K_0=1.2$, and $n=2$. ——, $\alpha=\frac{2}{3}$ or $\frac{4}{3}$; ·····, $\alpha=\infty$ or the δ-function model (23). When K_0 increases from 1.2 to 1.5, the curves move down, the shortest distance $\delta=0.8-y(r_m)$, and the curvature ϕ increases about 25–40 %.

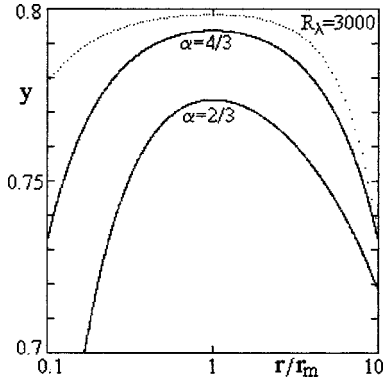

FIG. 3. As Fig. 2, but for $R_\lambda = 3000$.

better to express them in terms of R_λ. The method of calculating R_λ is described in [2] for the energy spectrum [9]

$$E(k) = K_0 \varepsilon^{2/3} k^{-5/3} F(k/k_d)/[1+(k_0/k)^{n+5/3}]. \quad (27)$$

The resultant R_λ is a function of $k_0/k_d = \eta k_0$. By using the $T(k)$ of [2] and Eqs. (8), (9), and (20), we determine the ratio $k_0/k_c = r_c k_0$, and we obtain

$$r_c/\eta = B R_\lambda^{3/2}. \quad (28)$$

The coefficient B depends on K_0 and n of Eq. (27): when $1 \leqslant n \leqslant 4$, $B = 0.041 \pm 0.006$ for $K_0 = 1.2$, $B = 0.029 \pm 0.005$ for $K_0 = 1.5$, and $B = 0.022 \pm 0.004$ for $K_0 = 1.8$. Finally, by using Eqs. (2)–(5), (24), and (28), we obtain the decay law (6) and

$$\mu = 6m/(3m+4), \quad (29a)$$

$$C_\delta = [1+4/(3m)]D, \quad C_\phi = 7.069(4/3+m)D, \quad (29b)$$

$$D = C_2^{3m/(3m+4)} (3mC_1/4)^{4/(3m+4)} / B^{4m/(3m+4)}. \quad (29c)$$

From Eqs. (22b) and (29a), we obtain $\mu \leqslant \frac{6}{5}$. The μ, C_δ, and C_ϕ for the most interesting cases $\alpha = \frac{2}{3}$ and $\frac{4}{3}$ are given in Table II. By using Eqs. (17b) and (24) and Table I, a linear-log plot of $-D_{LLL}(r)/\varepsilon r$ against r/r_m is given in Figs. 2 and 3 for $R_\lambda = 800$ and 3000, which clearly show that the FRN effect is important at experimental R_λ.

Many papers report $-D_{LLL}(r)/\varepsilon r$ obtained in experiments and simulations. For example, in Fig. 2 of Sreenivasan *et al.* [10], $-D_{LLL}(r)/\varepsilon r$ attains its maximum around $r/\eta = 10^2$, which is greater than 4/5. The maximum of $-D_{LLL}(r)/\varepsilon r$ is also greater than 4/5 in Figs. 10(b) and (11) of Anselmet *et al.* [5] and Fig. 16 of Saddoughi and Veeravalli [7]. However, according to Figs. 2 and 3 of this paper, the maximum of $-D_{LLL}(r)/\varepsilon r$ should be less than 4/5 in the scaling range. In plotting Fig. 16 of [7], Saddoughi and Veeravalli determine the dissipation ε by Eq. (1), in other words, they assume that the FRN effect is negligible in the scaling range around $r/\eta = 10^2$ at $R_\lambda = 600-1450$. They found that their $\varepsilon = -5D_{LLL}(r)/(4r)$ is substantially lower than the ε determined by the one-dimensional (1D) energy spectrum and did not give an explanation [7]. In fact, the FRN effect cannot be neglected and Eq. (1) is not valid at $R_\lambda = 600-1450$, so $-5D_{LLL}(r)/(4r)$ is substantially lower than the dissipation ε. If the ε determined by the 1D energy spectrum is used in plotting Fig. 16 of [7], the maximum of $-D_{LLL}(r)/\varepsilon r$ will be substantially less than 4/5, in agreement with our results.

Let us make a summary. Kolmogorov's 4/5 law (1) is valid in the inertial range corresponding to infinite R_λ. When R_λ is high but finite, $D_{LLL}(r)$ is given by Eq. (24) in the scaling range, and the constants C_1 and C_2 in Eq. (24) are given by Table I and Eq. (17b); since $C_1 > 0$ and $C_2 > 0$, $-D_{LLL}(r)/\varepsilon r$ must be less than 4/5 and changes with r in the scaling range, so the scaling $D_{LLL}(r) \sim r$ is not exact. From the exact spectral equations, we derive the decay law (6) and (29) of the FRN effect and determine all relevant constants so that the quantitative prediction of the FRN effect is feasible. The decay exponent $\mu \leqslant \frac{6}{5}$, its upper limit case of ($\alpha = \infty$, $m = 2$, $\mu = \frac{6}{5}$) corresponds to the δ-function model of energy input at large scales, and $\frac{2}{3} \leqslant \mu \leqslant 1$ for typical fully developed turbulent flows. The FRN effect decays slowly and cannot be neglected at experimental R_λ, as shown in Figs. 2 and 3. Hence, the scaling range (which is commonly called the inertial range in the literature) observed in experiments or simulations is not the real inertial range, which calls for reexamining the interpretation of the so-called inertial range data of experiments and simulations. An interesting example is that some experimental and numerical data (which were previously interpreted as the evidence of anomalous scaling) actually favor the normal scaling of turbulence, and the anomalous scaling is a consequence of the FRN effect [4].

The work was supported by the Natural Science Foundation of China and the research program ''Non-linear Scienc.''

[1] R. H. Kraichnan, Proc. R. Soc. London, Ser. A **434**, 65 (1991).
[2] J. Qian, Phys. Rev. E **55**, 337 (1997).
[3] A. S. Monin and A. M. Yaglom, *Statistical Fluid Mechanics* (Cambridge University Press, Cambridge, 1975); M. Nelkin, Adv. Phys. **43**, 143 (1994); U. Frisch, *Turbulence: The Legacy of A. N. Kolmogorov* (Cambridge University Press, Cambridge, 1995).
[4] J. Qian, J. Phys. A **31**, 3193 (1998); Phys. Rev. E **58**, 7325 (1998).
[5] F. Anselmet, Y. Gagne, E. J. Hopfinger, and R. A. Antonia, J. Fluid Mech. **140**, 63 (1984); K. R. Sreenivasan and R. A. Antonia, Annu. Rev. Fluid Mech. **29**, 435 (1997).
[6] J. O. Hinze, *Turbulence*, 2nd ed. (McGraw-Hill, New York, 1975); G. K. Batchelor, *The Theory of Homogeneous Turbulence* (Cambridge University Press, New York, 1953); C. M. Tchen, J. Res. Natl. Bur. Stand. **50**, 51 (1953); Phys. Rev. **93**, 4 (1954).
[7] S. G. Saddoughi and S. V. Veeravalli, J. Fluid Mech. **268**, 333 (1994).
[8] J. L. Lumley, Phys. Fluids **7**, 190 (1964).
[9] D. C. Leslie and G. L. Quarini, J. Fluid Mech. **91**, 65 (1979); J. Qian, Phys. Fluids **29**, 2165 (1986).
[10] K. R. Screenivasan, S. I. Vainshtein, R. Bhiladvala, I. San Gil, S. Chen, and N. Cao, Phys. Rev. Lett. **77**, 1488 (1996).